

# Renormalization Group Running of Lepton Mixing Parameters in See-Saw Models with $S_4$ Flavor Symmetry

Gui-Jun Ding<sup>a,b</sup>, Dong-Mei Pan<sup>a</sup>

<sup>a</sup>*Department of Modern Physics,  
University of Science and Technology of China, Hefei, Anhui 230026, China*

<sup>b</sup>*Department of Physics,  
University of Wisconsin-Madison, 1150 University Avenue, Madison, WI 53706, USA*

## Abstract

We study the renormalization group running of the tri-bimaximal mixing predicted by the two typical  $S_4$  flavor models at leading order. Although the textures of the mass matrices are completely different, the evolution of neutrino mass and mixing parameters is found to display approximately the same pattern. For both normal hierarchy and inverted hierarchy spectrum, the quantum corrections to both atmospheric and reactor neutrino mixing angles are so small that they can be neglected. The evolution of the solar mixing angle  $\theta_{12}$  depends on  $\tan \beta$  and neutrino mass spectrum, the deviation from its tri-bimaximal value could be large. Taking into account the renormalization group running effect, the neutrino spectrum is constrained by experimental data on  $\theta_{12}$  in addition to the self-consistency conditions of the models, and the inverted hierarchy spectrum is disfavored for large  $\tan \beta$ . The evolution of light-neutrino masses is approximately described by a common scaling factor.

# 1 Introduction

The neutrino physics has made great progress in the past decades. The mass square differences  $\Delta m_{\text{sol}}^2$ ,  $\Delta m_{\text{atm}}^2$  and the mixing angles have been measured with good accuracy [1, 2, 3]. A global fit to the current neutrino oscillation data demonstrates that the observed lepton mixing matrix is remarkably compatible with the tri-bimaximal (TB) mixing pattern [4], which suggests the following values of the mixing angles:

$$\sin^2 \theta_{12}^{TB} = \frac{1}{3}, \quad \sin^2 \theta_{23}^{TB} = \frac{1}{2}, \quad \sin \theta_{13}^{TB} = 0 \quad (1)$$

The question of how to achieve TB mixing has been the subject of intense theoretical speculation. Recently it has been found that the flavor symmetry based on the discrete group is particularly suitable to reproduce this specific mixing pattern in leading order (LO). Various discrete flavor symmetry models have been built, please see the Refs.[5, 6] for a review. A common feature of these model is to produce TB mixing at leading order, and the leading order predictions are always subjected to corrections due to higher dimensional operators in both the driving superpotential and the Yukawa superpotentials. These models provide an elegant description of neutrino mixing at very high energy scale, whereas the neutrino experiments are performed at low energy scale. In order to compare the model predictions with experimental data, one has to perform a renormalization group (RG) running from the high energy scale where the theory is defined to the electroweak scale  $M_Z$ . Moreover, we note that RG effects have interesting implications for model building, the lepton mixing angles can be magnified [7], even the bimaximal mixing at high energy can be compatible with low energy experiment [8]. Therefore, in a consistent flavor model building, we have to guarantee that the successful leading order predictions are not destroyed by the RG running corrections. The aim of this work is to analyze the RG corrections on the TB mixing pattern in two typical  $S_4$  flavor models [9, 10] in addition to the next to leading order corrections arising from high dimensional operators and to confront them with experimental values. We shall see that the running of the neutrino parameters is strongly constrained by the flavor symmetry as well, and this result holds very generally for the discrete flavor symmetry models.

The  $S_4$  flavor symmetry is very interesting. From the group theory point of view [11], it is the minimal group which can produce the TB mixing in a natural way, namely without ad hoc assumptions. It is remarkable that we have more alternatives to realize the exact TB mixing than those in the  $A_4$  flavor model [9, 10, 12, 13, 14, 15]. In particular, the **2** dimensional irreducible representation of  $S_4$  group can be utilized to describe the quark sector. Moreover, the group  $S_4$  as a flavor symmetry, as has been shown for example in Refs. [16, 17, 18, 19, 20], can also give a successful description of the quark and lepton masses and mixing angles within the framework of grand unified theory (GUT). We note that  $S_4$  as a flavor symmetry has been investigated long ago [21, 22], but with different aims and different results.

The paper is organized as follows. In section 2, we briefly review the RG equations for the type I see-saw mechanism. Then we give a concise introduction to the Bazzocchi-Merlo-Morisi (BMM)  $S_4$  model [9] and the  $S_4$  model of Ding [10] in section 3, where the main features of these models are shown. In section 4, Our results of RG effects on the neutrino mixing parameters for these two interesting models are presented. Finally we draw our conclusions in section 5.

## 2 Running of neutrino parameters in type I see-saw scenario

The running of neutrino masses and lepton mixing angles is very important and has been studied extensively in the literature [23, 24, 25, 26, 27, 28, 29, 30, 31, 32, 33] in the past years. In particular, Antusch et al. have developed the Mathematica package REAP in Ref. [30], which can solve renormalization group equations (RGE) and provide numerical values for the neutrino mass and mixing parameters. In this section, we present the RGEs for neutrino parameters in the minimal supersymmetric standard model (MSSM) extended by three singlet (right-handed) heavy neutrinos. The superpotential is given by

$$W = D^c Y_d Q H_d + U^c Y_u Q H_u + E^c Y_e L H_d + N^c Y_\nu L H_u + \frac{1}{2} N^c M N^c \quad (2)$$

where  $Q$  and  $L$  are the left-handed quark and lepton doublets chiral superfields, respectively,  $U^c$ ,  $D^c$ ,  $N^c$  and  $E^c$  are right-handed up-type quark, down-type quark, heavy neutrino and charged lepton singlet superfields, respectively,  $H_u$  and  $H_d$  are the well-known two Higgs doublets in MSSM. The Yukawa matrices  $Y_u$ ,  $Y_d$ ,  $Y_\nu$  and  $Y_e$  are general complex  $3 \times 3$  matrices and the  $3 \times 3$  heavy neutrino mass matrix  $M$  is symmetric. Integrating out all the heavy singlet neutrinos, one gets the usual dimension-5 effective neutrino mass operator

$$\mathcal{L}_\kappa = -\frac{1}{4} \kappa_{fg} (L^f \cdot H_u) (L^g \cdot H_u) \quad (3)$$

where  $f$  and  $g$  are family indices, and the dot indicates the  $SU(2)_L$  invariant contractions. After electroweak symmetry breaking, this operator leads to the light-neutrino masses

$$m_\nu(\mu) = -\frac{1}{4} \kappa(\mu) v^2 \sin^2 \beta \quad (4)$$

where  $\mu$  is the renormalization scale,  $v = 246$  GeV and  $\tan \beta = v_u/v_d$  is the ratio of vacuum expectation values (VEV) of the Higgs doublets. Above the heaviest neutrino mass scale, the light-neutrino mass matrix reads

$$m_\nu(\mu) = -\frac{1}{2} Y_\nu^T(\mu) M^{-1}(\mu) Y_\nu(\mu) v^2 \sin^2 \beta \quad (5)$$

When we evolved the energy from high energy scale down to the low experimental observation scale, the heavy singlet neutrinos involved in the see-saw mechanism have to be integrated out one by one, thus one has to consider a series of effective theories [30]. In general, the light-neutrino mass matrix can be written as<sup>1</sup>

$$m_\nu = -\frac{1}{4} \left( \kappa^{(n)} + 2 Y_\nu^{(n)T} M^{(n)-1} Y_\nu^{(n)} \right) v^2 \sin^2 \beta \quad (6)$$

where the superscript  $(n)$  denotes a quantity below the  $n$ th mass threshold. In the MSSM, the two parts  $\kappa^{(n)}$  and  $2 Y_\nu^{(n)T} M^{(n)-1} Y_\nu^{(n)}$  evolve in the same way

$$16\pi^2 \frac{dX^{(n)}}{dt} = \left( Y_e^\dagger Y_e + Y_\nu^{(n)\dagger} Y_\nu^{(n)} \right)^T X^{(n)} + X^{(n)} \left( Y_e^\dagger Y_e + Y_\nu^{(n)\dagger} Y_\nu^{(n)} \right) + \left[ 2 \text{Tr} (Y_\nu^{(n)\dagger} Y_\nu^{(n)} + 3 Y_u^\dagger Y_u) - \frac{6}{5} g_1^2 - 6 g_2^2 \right] X^{(n)} \quad (7)$$

---

<sup>1</sup>We use the GUT charge normalization for the gauge coupling  $g_1$ .

where  $t = \ln(\mu/\mu_0)$ , and  $X$  stands for  $\kappa^{(n)}$  or  $2Y_\nu^T M^{-1} Y_\nu^{(n)}$ . The RG equations for the Yukawa couplings  $Y_u, Y_d, Y_\nu, Y_e$  and the right-handed neutrino mass matrix  $M$  are given by

$$\begin{aligned}
16\pi^2 \frac{dY_\nu^{(n)}}{dt} &= Y_\nu^{(n)} \left[ 3Y_\nu^{(n)\dagger} Y_\nu^{(n)} + Y_e^\dagger Y_e + \text{Tr}(Y_\nu^{(n)\dagger} Y_\nu^{(n)}) + 3\text{Tr}(Y_u^\dagger Y_u) - \frac{3}{5}g_1^2 - 3g_2^2 \right] \\
16\pi^2 \frac{dY_e}{dt} &= Y_e \left[ 3Y_e^\dagger Y_e + Y_\nu^{(n)\dagger} Y_\nu^{(n)} + 3\text{Tr}(Y_d^\dagger Y_d) + \text{Tr}(Y_e^\dagger Y_e) - \frac{9}{5}g_1^2 - 3g_2^2 \right] \\
16\pi^2 \frac{dY_u}{dt} &= Y_u \left[ Y_d^\dagger Y_d + 3Y_u^\dagger Y_u + \text{Tr}(Y_\nu^{(n)\dagger} Y_\nu^{(n)}) + 3\text{Tr}(Y_u^\dagger Y_u) - \frac{13}{15}g_1^2 - 3g_2^2 - \frac{16}{3}g_3^2 \right] \\
16\pi^2 \frac{dY_d}{dt} &= Y_d \left[ 3Y_d^\dagger Y_d + Y_u^\dagger Y_u + 3\text{Tr}(Y_d^\dagger Y_d) + \text{Tr}(Y_e^\dagger Y_e) - \frac{7}{15}g_1^2 - 3g_2^2 - \frac{16}{3}g_3^2 \right] \\
16\pi^2 \frac{dM^{(n)}}{dt} &= 2(Y_\nu Y_\nu^\dagger)^{(n)} M + 2M(Y_\nu Y_\nu^\dagger)^{(n)T} \quad (8)
\end{aligned}$$

In the full theory above the highest see-saw scale, the superscript  $(n)$  has to be omitted, and the RG equations for MSSM without singlet neutrinos can be recovered by setting the neutrino Yukawa couplings and the mass matrix of the singlets to be zero. Below the SUSY breaking scale, which is taken to be 1000 GeV in this work, we go to the standard model region. Since all the heavy right-handed neutrinos have already been integrated out at this scale, the neutrino masses are described by the effective dimension-5 operator, and the neutrino mass matrix  $m_\nu$  evolves as

$$16\pi^2 \frac{dm_\nu}{dt} = -\frac{3}{2}(Y_e^\dagger Y_e)^T m_\nu - \frac{3}{2}m_\nu(Y_e^\dagger Y_e) + \left[ 2\text{Tr}(3Y_u^\dagger Y_u + 3Y_d^\dagger Y_d + Y_e^\dagger Y_e) - 3g_2^2 + \lambda \right] m_\nu \quad (9)$$

where  $\lambda$  is the Higgs self-interaction coupling<sup>2</sup>. In order to calculate the RG evolution of the effective neutrino mass matrix, we have to solve the RG equations for all the parameters of the theory simultaneously<sup>3</sup>. At the mass threshold, we should integrate out the corresponding heavy neutrino and perform the tree-level matching condition for the effective coupling constant between the effective theories

$$\kappa_{gf}^{(n)} \Big|_{M_n} = \kappa_{gf}^{(n+1)} \Big|_{M_n} + 2 \left( Y_\nu^{(n+1)T} \right)_{gn} M_n^{-1} \left( Y_\nu^{(n+1)} \right)_{nf} \Big|_{M_n} \quad (\text{no sum over } n) \quad (10)$$

### 3 Variants of the Two $S_4$ Models

In this section, we recapitulate the main features of the  $S_4$  flavor model of BMM [9] and Ding [10]. Both models generate neutrino masses via type I see-saw mechanism, and the neutrino TB mixing is produced at LO. For an introduction to the group theory of  $S_4$  we refer to Refs.[10, 20], the same conventions for the  $S_4$  representation matrix and Clebsch-Gordan coefficient are used in this work.

<sup>2</sup>We use the convention that the Higgs self-interaction term in the Lagrangian is  $-\frac{\lambda}{4}(H^\dagger H)^2$ .

<sup>3</sup>The running of the gauge couplings has to be taken into account as well, the corresponding  $\beta$  functions are well-known .

### 3.1 BMM $S_4$ model

In this model the flavor symmetry  $S_4$  is accompanied by the cyclic group  $Z_5$  and the Froggatt-Nielsen symmetry  $U(1)_{FN}$ . The  $S_4$  flavor symmetry is spontaneously broken to the subgroup  $Z_2 \times Z_2$  in the neutrino sector and to nothing in the charged lepton one at leading order. This misalignment between the flavor symmetry breaking in the neutrino and charged lepton sectors is exactly the origin of the TB mixing. Furthermore, the auxiliary symmetry  $Z_5$  eliminating some dangerous terms, with the interplay of the continuous  $U(1)_{FN}$ , is responsible for the hierarchy among the charged lepton masses. The leptonic fields and the flavon fields of the model and their transformation properties under the flavor symmetry are shown in Table 1.

	$\ell$	$e^c$	$\mu^c$	$\tau^c$	$\nu^c$	$H_{u,d}$	$\theta$	$\psi$	$\eta$	$\Delta$	$\varphi$	$\xi'$
$S_4$	$3_1$	$1_2$	$1_2$	$1_1$	$3_1$	$1_1$	$1_1$	$3_1$	$2$	$3_1$	$2$	$1_2$
$Z_5$	$\omega^4$	$1$	$\omega^2$	$\omega^4$	$\omega$	$1$	$1$	$\omega^2$	$\omega^2$	$\omega^3$	$\omega^3$	$1$
$U(1)_{FN}$	$0$	$1$	$0$	$0$	$0$	$0$	$-1$	$0$	$0$	$0$	$0$	$0$

Table 1: Transformation properties of the leptonic fields and flavons in the BMM model [9]. Note that  $\omega$  is the fifth root of unity, i.e.  $\omega = e^{i2\pi/5}$ .

By introducing a  $U(1)_R$  symmetry, the authors in Ref. [9] have shown that the flavon fields develop the following vacuum alignment at LO

$$\begin{aligned}
\langle \psi \rangle &= \begin{pmatrix} 0 \\ 1 \\ 0 \end{pmatrix} v_\psi, & \langle \eta \rangle &= \begin{pmatrix} 0 \\ 1 \end{pmatrix} v_\eta \\
\langle \Delta \rangle &= \begin{pmatrix} 1 \\ 1 \\ 1 \end{pmatrix} v_\Delta, & \langle \varphi \rangle &= \begin{pmatrix} 1 \\ 1 \end{pmatrix} v_\varphi \\
\langle \xi' \rangle &= v_{\xi'}, & \langle \theta \rangle &= v_\theta
\end{aligned} \tag{11}$$

The superpotential of the model in the lepton sector is

$$\begin{aligned}
w_\ell &= \sum_{i=1}^4 \frac{\theta}{\Lambda} \frac{y_{e,i}}{\Lambda^3} e^c (\ell X_i)_{1_2} H_d + \frac{y_\mu}{\Lambda^2} \mu^c (\ell \psi \eta)_{1_2} H_d + \frac{y_\tau}{\Lambda} \tau^c (\ell \psi)_{1_1} H_d + \dots \\
w_\nu &= y(\nu^c \ell)_{1_1} H_u + x_d(\nu^c \nu^c \varphi)_{1_1} + x_t(\nu^c \nu^c \Delta)_{1_1} + \dots
\end{aligned} \tag{12}$$

where the subscript  $1_1$  and  $1_2$  denote the contraction in  $1_1$  and  $1_2$ , respectively, and dots stand for higher dimensional operators, which are suppressed by additional powers of the cutoff  $\Lambda$ . The composite  $X$  is given by

$$X = \{\psi \psi \eta, \psi \eta \eta, \Delta \Delta \xi', \Delta \varphi \xi'\} \tag{13}$$

Taking into account the vacuum alignment in Eq.(11), the mass matrix for the charged lepton reads

$$m_\ell = \frac{v_d u}{\sqrt{2}} \begin{pmatrix} y_e^{(1)} u^2 t & y_e^{(2)} u^2 t & y_e^{(3)} u^2 t \\ 0 & y_\mu u & 0 \\ 0 & 0 & y_\tau \end{pmatrix} \tag{14}$$

where  $y_e^{(i)}$  is the linear combination of the  $y_{e,i}$  contributions. The parameter  $u$  parameterizes the ratio  $v_\psi/\Lambda$ ,  $v_\eta/\Lambda$ ,  $v_\Delta/\Lambda$ ,  $v_\varphi/\Lambda$  and  $v_{\xi'}/\Lambda$ , which should be of the same order of magnitude to produce the mass hierarchy among the charged fermions. The parameter  $t$  denotes the ratio  $v_\theta/\Lambda$ . It has been shown that the parameters  $u$  and  $t$  belong to the range  $0.01 < u, t < 0.05$  [9]. The first term in  $w_\nu$  is the neutrino Dirac-Yukawa coupling, and the last two terms determine the mass matrix of the heavy right-handed neutrinos. Straightforwardly we have

$$m_\nu^D = \frac{1}{\sqrt{2}} \begin{pmatrix} 1 & 0 & 0 \\ 0 & 0 & 1 \\ 0 & 1 & 0 \end{pmatrix} y v_u, \quad M_N = \begin{pmatrix} 2c & b-c & b-c \\ b-c & b+2c & -c \\ b-c & -c & b+2c \end{pmatrix} \quad (15)$$

where  $b = 2x_d v_\varphi$  and  $x_t = 2x_t v_\Delta$ . Integrating out the heavy neutrino  $\nu^c$ , the light-neutrino effective mass matrix is given by the see-saw formula

$$m_\nu = -(m_\nu^D)^T M_N^{-1} m_\nu^D = \frac{y^2 v_u^2}{4} \begin{pmatrix} \frac{b+c}{b(b-3c)} & \frac{-b+c}{b(b-3c)} & \frac{-b+c}{b(b-3c)} \\ \frac{-b+c}{b(b-3c)} & \frac{-b^2+4bc+3c^2}{b(b^2-9c^2)} & \frac{b^2-2bc+3c^2}{b(b^2-9c^2)} \\ \frac{-b+c}{b(b-3c)} & \frac{b^2-2bc+3c^2}{b(b^2-9c^2)} & \frac{-b^2+4bc+3c^2}{b(b^2-9c^2)} \end{pmatrix}$$

The light-neutrino mass matrix  $m_\nu$  can be diagonalized by

$$U_\nu^T m_\nu U_\nu = \text{diag}(m_{\nu_1}, m_{\nu_2}, m_{\nu_3}) \quad (16)$$

where  $m_{\nu_1, \nu_2, \nu_3}$  are the light-neutrino masses

$$\begin{aligned} m_{\nu_1} &= \frac{y^2 v_u^2}{2} \frac{1}{|-b+3c|} \\ m_{\nu_2} &= \frac{y^2 v_u^2}{2} \frac{1}{2|b|} \\ m_{\nu_3} &= \frac{y^2 v_u^2}{2} \frac{1}{|b+3c|} \end{aligned} \quad (17)$$

The unitary matrix  $U_\nu$  can be written as

$$U_\nu = i U_{TB} U_P \quad (18)$$

where  $U_{TB}$  is the TB mixing matrix

$$U_{TB} = \begin{pmatrix} \sqrt{2/3} & 1/\sqrt{3} & 0 \\ -1/\sqrt{6} & 1/\sqrt{3} & 1/\sqrt{2} \\ -1/\sqrt{6} & 1/\sqrt{3} & -1/\sqrt{2} \end{pmatrix} \quad (19)$$

and  $U_P = \text{diag}(e^{i\alpha_1/2}, e^{i\alpha_2/2}, e^{i\alpha_3/2})$  is a matrix of phase with  $\alpha_1 = \arg(-b+3c)$ ,  $\alpha_2 = \arg(b)$  and  $\alpha_3 = \arg(b+3c)$ . Therefore the lepton mixing matrix is the TB mixing apart from the negligible corrections of order  $u^2 t^2$  from the charged lepton sector. We note that the right-handed neutrino mass matrix  $M_N$  is diagonalized by TB mixing as well, the mass eigenvalues are given by  $M_1 = |-b+3c|$ ,  $M_2 = 2|b|$  and  $M_3 = |b+3c|$ . Comparing with the light-neutrino masses in Eq.(15), we have the interesting relation

$$m_{\nu_i} = \frac{y^2 v_u^2}{2M_i} \quad (20)$$

The Yukawa coupling  $y$  is of  $\mathcal{O}(1)$ , and we use  $|\Delta m_{atm}^2|^{1/2}$  as the typical light-neutrino mass scale, then we obtain

$$M_i \sim 10^{14 \div 15} \text{GeV} \quad (21)$$

The coefficients  $x_t$  and  $x_d$  are expected to be of  $\mathcal{O}(1)$ , as a consequence the VEVs  $v_\varphi$  and  $v_\Delta$  should be of the same order as the right-handed neutrino mass  $M_i$ . It is obvious that the model is rather constrained, there are only three independent parameters, which can be chosen to be  $|b| = y^2 v_u^2 / (4m_{\nu 2})$ ,  $Z$  and  $\Omega$ . The latter two are defined according to

$$\frac{c}{b} = Z e^{i\Omega} \quad (22)$$

We can easily express  $Z$  and  $\Omega$  in terms of the neutrino masses as

$$Z = \frac{1}{3} \sqrt{\frac{2m_{\nu 2}^2}{m_{\nu 1}^2} + \frac{2m_{\nu 2}^2}{m_{\nu 3}^2} - 1}$$

$$\cos \Omega = \frac{\frac{m_{\nu 2}^2}{m_{\nu 3}^2} - \frac{m_{\nu 2}^2}{m_{\nu 1}^2}}{\sqrt{\frac{2m_{\nu 2}^2}{m_{\nu 1}^2} + \frac{2m_{\nu 2}^2}{m_{\nu 3}^2} - 1}} \quad (23)$$

The above relations hold for both normal hierarchy (NH) and inverted hierarchy (IH) spectrum. Taking into account the experimentally measured mass difference  $\Delta m_{sol}^2 = m_{\nu 2}^2 - m_{\nu 1}^2$  and  $\Delta m_{atm}^2 = |m_{\nu 3}^2 - m_{\nu 1}^2|$ , we have only one free parameter left, which is conveniently chosen to be the lightest neutrino mass. Imposing the constraint  $|\cos \Omega| \leq 1$ , we obtain the following limits for the lightest neutrino mass <sup>4</sup>

$$\begin{aligned} m_{\nu 1} &\geq 0.011 \text{ eV}, & \text{NH} \\ m_{\nu 3} &\geq 0.029 \text{ eV}, & \text{IH} \end{aligned} \quad (24)$$

where the central values of  $\Delta m_{sol}^2$  and  $\Delta m_{atm}^2$  are used. We would like to stress that the mass squared differences are running quantities, therefore the bounds in Eq.(24) would change somewhat at low energy after considering the RG effects.

The model is so predictive that we can express the Majorana phases in terms of the lightest neutrino mass as well. In the standard parametrization [35], the lepton PMNS mixing matrix is defined by

$$U_{PMNS} = \text{diag}(e^{i\delta_e}, e^{i\delta_\mu}, e^{i\delta_\tau}) \begin{pmatrix} c_{12}c_{13} & s_{12}c_{13} & s_{13}e^{-i\delta} \\ -s_{12}c_{23} - c_{12}s_{23}s_{13}e^{i\delta} & c_{12}c_{23} - s_{12}s_{23}s_{13}e^{i\delta} & s_{23}c_{13} \\ s_{12}s_{23} - c_{12}c_{23}s_{13}e^{i\delta} & -c_{12}s_{23} - s_{12}c_{23}s_{13}e^{i\delta} & c_{23}c_{13} \end{pmatrix}$$

$$\times \text{diag}(e^{-i\varphi_1/2}, e^{-i\varphi_2/2}, 1) \quad (25)$$

where  $c_{ij} = \cos \theta_{ij}$ ,  $s_{ij} = \sin \theta_{ij}$  with  $\theta_{ij} \in [0, \pi/2]$ , the unphysical phases  $\delta_e$ ,  $\delta_\mu$  and  $\delta_\tau$  can be absorbed into charged lepton fields,  $\delta$  is the Dirac CP violating phase,  $\alpha_{21}$  and  $\alpha_{31}$  are the two Majorana CP violating phases, all the three CP violating phases  $\delta$ ,  $\varphi_1$  and  $\varphi_2$  are allowed to vary in the range of  $0 \sim 2\pi$ . Recalling that the leptonic mixing matrix is given by Eq.(18), we can identify the two CP violating phases as

$$\varphi_1 = \alpha_3 - \alpha_1, \quad \varphi_2 = \alpha_3 - \alpha_2 \quad (26)$$

---

<sup>4</sup>The same parameter space is obtained by the neutrino mass sum rule method [34].

As a result, we have

$$\begin{aligned}\cos \varphi_1 &= \frac{-1 + 9Z^2}{\sqrt{1 + 81Z^4 - 18Z^2 \cos 2\Omega}}, & \sin \varphi_1 &= \frac{-6Z \sin \Omega}{\sqrt{1 + 81Z^4 - 18Z^2 \cos 2\Omega}} \\ \cos \varphi_2 &= \frac{1 + 3Z \cos \Omega}{\sqrt{1 + 9Z^2 + 6Z \cos \Omega}}, & \sin \varphi_2 &= \frac{3Z \sin \Omega}{\sqrt{1 + 9Z^2 + 6Z \cos \Omega}}\end{aligned}\quad (27)$$

Since we can only determine  $\cos \Omega$  from the neutrino mass spectrum, the Majorana phases  $\varphi_1, \varphi_2$  can take two sets of values corresponding to  $\sin \Omega > 0$  and  $\sin \Omega < 0$  respectively. We note that the Dirac CP phase is undetermined because the reactor angle is vanishing in TB mixing. The above successful leading order results are corrected by the NLO contributions, which consists of the higher dimensional operators in both the driving superpotential and Yukawa superpotentials. It has been shown that all the three leptonic mixing angles receive corrections of order  $u$  [9].

### 3.2 The $S_4$ model of Ding

The total flavor symmetry of this model is  $S_4 \times Z_3 \times Z_4$  [10]. It is remarkable that the realistic pattern of fermion masses and flavor mixing in both the lepton and quark sector have been reproduced in this model, and the mass hierarchies are determined by the spontaneous breaking of the flavor symmetry without invoking a Froggatt-Nielsen  $U(1)$  symmetry. The leptonic fields and the flavons of the model and their classifications under the flavor symmetry are shown in Table 2, where the quark fields have been omitted.

	$\ell$	$e^c$	$\mu^c$	$\tau^c$	$\nu^c$	$H_{u,d}$	$\varphi$	$\chi$	$\zeta$	$\eta$	$\phi$	$\Delta$
$S_4$	$3_1$	$1_1$	$1_2$	$1_1$	$3_1$	$1_1$	$3_1$	$3_2$	$1_2$	$2$	$3_1$	$1_2$
$Z_3$	$\omega$	$\omega^2$	$\omega^2$	$\omega^2$	$1$	$1$	$1$	$1$	$1$	$\omega^2$	$\omega^2$	$\omega^2$
$Z_4$	$1$	$i$	$-1$	$-i$	$1$	$1$	$i$	$i$	$1$	$1$	$1$	$-1$

Table 2: The transformation rules of the leptonic fields and the flavons under the symmetry groups  $S_4$ ,  $Z_3$  and  $Z_4$  in the  $S_4$  model of Ref. [10], where  $\omega$  is the third root of unity, i.e.  $\omega = e^{i\frac{2\pi}{3}} = (-1 + i\sqrt{3})/2$ .

In this model the  $S_4$  symmetry is broken down to Klein four and  $Z_3$  subgroups in the neutrino and charged lepton sector, respectively, at LO, this specific breaking scheme require flavon fields develop the following vacuum configuration

$$\begin{aligned}\langle \varphi \rangle &= (0, V_\varphi, 0), & \langle \chi \rangle &= (0, V_\chi, 0) & \langle \zeta \rangle &= V_\zeta \\ \langle \eta \rangle &= (V_\eta, V_\eta), & \langle \phi \rangle &= (V_\phi, V_\phi, V_\phi), & \langle \Delta \rangle &= V_\Delta\end{aligned}\quad (28)$$

We have demonstrated that this particular vacuum alignment is a natural solution to the scalar potential, all the VEVs (scaled by the cutoff  $\Lambda$ )  $V_\varphi/\Lambda$ ,  $V_\chi/\Lambda$ ,  $V_\zeta/\Lambda$ ,  $V_\eta/\Lambda$ ,  $V_\phi/\Lambda$  and  $V_\Delta/\Lambda$  are of the same order of magnitude about  $\mathcal{O}(\lambda_c^2)$ , and this vacuum configuration is stable under the higher order corrections, please see Ref. [10] for detail. Then the most general superpotential in the lepton sector, which is compatible with the representation assignment of Table 2, is given



by

$$\begin{aligned}
w_\ell &= \frac{y_{e1}}{\Lambda^3} e^c(\ell\varphi)_{11}(\varphi\varphi)_{11}h_d + \frac{y_{e2}}{\Lambda^3} e^c((\ell\varphi)_2(\varphi\varphi)_2)_{11}h_d + \frac{y_{e3}}{\Lambda^3} e^c((\ell\varphi)_{31}(\varphi\varphi)_{31})_{11}h_d \\
&+ \frac{y_{e4}}{\Lambda^3} e^c((\ell\chi)_2(\chi\chi)_2)_{11}h_d + \frac{y_{e5}}{\Lambda^3} e^c((\ell\chi)_{31}(\chi\chi)_{31})_{11}h_d + \frac{y_{e6}}{\Lambda^3} e^c(\ell\varphi)_{11}(\chi\chi)_{11}h_d \\
&+ \frac{y_{e7}}{\Lambda^3} e^c((\ell\varphi)_2(\chi\chi)_2)_{11}h_d + \frac{y_{e8}}{\Lambda^3} e^c((\ell\varphi)_{31}(\chi\chi)_{31})_{11}h_d + \frac{y_{e9}}{\Lambda^3} e^c((\ell\chi)_2(\varphi\varphi)_2)_{11}h_d \\
&+ \frac{y_{e10}}{\Lambda^3} e^c((\ell\chi)_{31}(\varphi\varphi)_{31})_{11}h_d + \frac{y_\mu}{2\Lambda^2} \mu^c(\ell(\varphi\chi)_{32})_{12}h_d + \frac{y_\tau}{\Lambda} \tau^c(\ell\varphi)_{11}h_d + \dots \\
w_\nu &= \frac{y_{\nu 1}}{\Lambda} ((\nu^c\ell)_2\eta)_{11}h_u + \frac{y_{\nu 2}}{\Lambda} ((\nu^c\ell)_{31}\phi)_{11}h_u + \frac{1}{2}M(\nu^c\nu^c)_{11} + \dots
\end{aligned} \tag{29}$$

where  $(\dots)_{11,12,2,31,32}$  stands for the  $1_1$ ,  $1_2$ ,  $2$ ,  $3_1$  and  $3_2$  products, respectively. We note that and one can always set  $M$  to be real and positive by global phase transformation of the lepton fields, and a priori  $M$  should be of the same order as the cutoff scale  $\Lambda$ . Taking into account the vacuum alignment in Eq.(28), we find that the charged lepton mass matrix is diagonal at LO,

$$m_\ell = \frac{v_d}{\sqrt{2}} \begin{pmatrix} y_e \frac{v_\varphi^3}{\Lambda^3} & 0 & 0 \\ 0 & y_\mu \frac{v_\varphi v_\chi}{\Lambda^2} & 0 \\ 0 & 0 & y_\tau \frac{v_\varphi}{\Lambda} \end{pmatrix} \tag{30}$$

where  $y_e$  is the result of all the different contributions of  $y_{e_i}$ . The neutrino Dirac and Majorana mass matrices can be straightforwardly read out as

$$m_\nu^D = \frac{v_u}{\sqrt{2}} \begin{pmatrix} 2b & a-b & a-b \\ a-b & a+2b & -b \\ a-b & -b & a+2b \end{pmatrix}, \quad M_N = \begin{pmatrix} M & 0 & 0 \\ 0 & 0 & M \\ 0 & M & 0 \end{pmatrix} \tag{31}$$

where  $a = y_{\nu 1} \frac{v_\eta}{\Lambda}$  and  $b = y_{\nu 2} \frac{v_\phi}{\Lambda}$ . As a result, the light-neutrino mass matrix is given by

$$m_\nu = -(m_\nu^D)^T M_N^{-1} m_\nu^D = -\frac{v_u^2}{2M} \begin{pmatrix} 2a^2 - 4ab + 6b^2 & a^2 + 2ab - 3b^2 & a^2 + 2ab - 3b^2 \\ a^2 + 2ab - 3b^2 & a^2 - 4ab - 3b^2 & 2a^2 + 2ab + 6b^2 \\ a^2 + 2ab - 3b^2 & 2a^2 + 2ab + 6b^2 & a^2 - 4ab - 3b^2 \end{pmatrix} \tag{32}$$

We can see that the mass matrix  $m_\nu$  is exactly diagonalized by the TB mixing matrix

$$U_\nu^T m_\nu U_\nu = \text{diag}(m_{\nu 1}, m_{\nu 2}, m_{\nu 3}) \tag{33}$$

The unitary matrix  $U_\nu$  is

$$U_\nu = U_{TB} \text{diag}(e^{-i\alpha_1/2}, e^{-i\alpha_2/2}, e^{-i\alpha_3/2}) \tag{34}$$

The phases  $\alpha_1$ ,  $\alpha_2$  and  $\alpha_3$  are closely related to the Majorana phase

$$\alpha_1 = \arg(-(a-3b)^2/M), \quad \alpha_2 = \arg(-4a^2/M), \quad \alpha_3 = \arg((a+3b)^2/M) \tag{35}$$

and the neutrino masses are given by

$$m_{\nu 1} = |(a-3b)^2|v_u^2/(2M), \quad m_{\nu 2} = 2|a|^2v_u^2/M, \quad m_{\nu 3} = |(a+3b)^2|v_u^2/(2M) \tag{36}$$

It is interesting to estimate the order of magnitude for the right-handed neutrino mass  $M$ . Since the parameters  $a$  and  $b$  are expected to be of order  $\lambda_c^2$ , with this and using  $\sqrt{|\Delta m_{atm}^2|} \simeq 0.05$  eV as the light-neutrino mass scale in the see-saw formula, we obtain

$$M \sim 10^{12/13} \text{GeV} \quad (37)$$

Similar to the analysis of section 3.1, we define

$$\frac{b}{a} = R e^{i\Phi} \quad (38)$$

Straightforwardly we can express  $R$  and  $\cos \Phi$  as functions of the neutrino masses

$$R = \frac{1}{3} \sqrt{\frac{2m_{\nu 1}}{m_{\nu 2}} + \frac{2m_{\nu 3}}{m_{\nu 2}} - 1}$$

$$\cos \Phi = \frac{\frac{m_{\nu 3}}{m_{\nu 2}} - \frac{m_{\nu 1}}{m_{\nu 2}}}{\sqrt{\frac{2m_{\nu 1}}{m_{\nu 2}} + \frac{2m_{\nu 3}}{m_{\nu 2}} - 1}} \quad (39)$$

In exactly the same way section 3.1, the Majorana phases in standard parameterization are determined as

$$\varphi_1 = \alpha_1 - \alpha_3, \quad \varphi_2 = \alpha_2 - \alpha_3 \quad (40)$$

with

$$\cos \varphi_1 = \frac{-(1 - 9R^2)^2 + 36R^2 \sin^2 \Phi}{(1 + 9R^2)^2 - 36R^2 \cos^2 \Phi}, \quad \sin \varphi_1 = \frac{12R(1 - 9R^2) \sin \Phi}{(1 + 9R^2)^2 - 36R^2 \cos^2 \Phi}$$

$$\cos \varphi_2 = \frac{-1 - 9R^2 \cos 2\Phi - 6R \cos \Phi}{1 + 9R^2 + 6R \cos \Phi}, \quad \sin \varphi_2 = \frac{6R(1 + 3R \cos \Phi) \sin \Phi}{1 + 9R^2 + 6R \cos \Phi} \quad (41)$$

Consequently, all the low energy parameters in the neutrino sector can be expressed in terms of the lightest neutrino mass. Imposing the condition  $|\cos \Phi| \leq 1$ , we get the following constraint on the lightest neutrino mass:

$$m_{\nu 1} \geq 0.011 \text{ eV}, \quad \text{NH}$$

$$m_{\nu 3} > 0.0 \text{ eV}, \quad \text{IH} \quad (42)$$

The NLO corrections have been analyzed in detail in Ref. [10]. It is shown that both the neutrino masses and mixing angles receive corrections of order  $\varepsilon \sim \lambda_c^2$  with respect to leading order result, where  $\varepsilon$  parameterizes the ratio  $VEV/\Lambda$  and  $\lambda_c$  is the Cabibbo angle.

## 4 RG running effects in $S_4$ flavor models

As has been shown, the TB mixing is achieved in both BMM model and the  $S_4$  model of Ding at LO. In this section, we turn to a quantitative discussion of RG effects, and compare them with the NLO corrections and the experimental data. For definiteness we shall assume a supersymmetry breaking scale of 1 TeV, below which the SM is valid. We note that the mass hierarchy between top and bottom is produced via the spontaneous breaking of flavor symmetry in both models, and  $\tan \beta$  should be small. As a result, we shall take the parameter  $\tan \beta$  to be 10 apart except where explicitly indicated otherwise. To study the running of the neutrino

mixing parameters from the GUT scale to the electroweak scale, the Mathematica package REAP is used [30]. This package numerically solves the RG equations of the quantities relevant for neutrino mass and mixing, and it has been widely used for different purposes [36]. The package can be downloaded from <http://users.physik.tu-muenchen.de/rge/REAP/index.html>, and Mathematica version 5 or higher is required. We note that the approximate analytical solutions based on leading log approximation to the RG equations have been derived in Refs.[29, 30], which allows one to understand the generic behavior of the renormalization effects. However, due to enhancement/suppression factors and possible cancelations, the exact numerical solutions may differ considerably from those estimates. Therefore throughout this paper we adopt a numerical approach, exploiting the convenient REAP package.

As has been demonstrated above, we generally need to introduce flavon fields to break the flavor symmetry in order to generate fermion masses and flavor mixing. In the unbroken phase of flavor symmetry, the flavons are active fields, therefore the corresponding RG equations should be modified in principle. However, the superpotentials of the models in Eq.(12) and Eq.(29) contain all the possible LO terms allowed by the symmetries, the invariance under the flavor symmetry  $S_4$  is maintained until we move down to the scale of the VEV of the flavon fields, which is of the order of GUT scale. We conclude that the flavor structures of the models are preserved above the scale of the VEV of the flavon fields, the contributions of the flavon fields in the RG running can be absorbed by the redefinition of the model parameters [38]. In the following, we will discuss the RG evolution of neutrino masses and mixing parameters in both  $S_4$  flavor models, starting from the initial conditions of neutrino Dirac and Majorana mass matrices described in section 3 at the GUT scale. In particular, the parameter spaces are scanned.

#### 4.1 RG effects in the BMM models

In this section we report results of the calculations of the RG evolution of the neutrino mixing parameters in the BMM model. Without loss of generality, we choose the Yukawa coupling  $y = 1$  for our numerical analysis. The GUT scale neutrino mass squared differences  $m_{\nu 2}^2 - m_{\nu 1}^2$  and  $|m_{\nu 3}^2 - m_{\nu 1}^2|$  are treated as random numbers in the range of  $3.5 \times 10^{-5} \text{ eV}^2 \sim 2.5 \times 10^{-4} \text{ eV}^2$  and  $1.0 \times 10^{-3} \text{ eV}^2 \sim 8.3 \times 10^{-3} \text{ eV}^2$  respectively,<sup>5</sup> and the lightest neutrino mass is varied from the lowest bound determined by Eq.(23) or Eq.(39) to 0.2 eV which is the future sensitivity of KATRIN experiment [37]. The RG corrected neutrino mixing angles as functions of the lightest neutrino mass are shown in Fig. 1 for both NH and IH spectrum<sup>6</sup>. These plots display only the points corresponding to choices of the parameters reproducing  $\Delta m_{\text{atm}}^2$ ,  $\Delta m_{\text{sol}}^2$  and the mixing angles within the  $3\sigma$  interval.

We see that the lightest neutrino mass is still bounded from below, and the concrete values of the lower bounds are about 0.0107 eV and 0.027 eV, respectively, for the NH and IH spectrum, and these values are found to be almost independent of  $\tan \beta$ . It is remarkable that all the mixing parameters and  $J_{CP}$  are predicted to lie in a relative narrow range. For both NH and IH spectrum, it is obvious that the RG changes of the atmospheric and reactor angles are very small, the corresponding allowed regions lie within the current  $1\sigma$  bounds. In particular, the RG corrections to  $\sin^2 \theta_{23}$  and  $\sin^2 \theta_{13}$  are of the same order or even smaller than the NLO contributions. On the other hand, the running of the solar neutrino mixing angle displays a

<sup>5</sup>We shall show later that the mass squared difference at the GUT scale is about a factor of  $1.2 \sim 3$  larger than its low energy value in the whole spectrum.

<sup>6</sup>The results are independent of the sign of  $\sin \Omega$ , the reason is explained later.

different pattern. The RG change of  $\sin^2 \theta_{12}$  is much larger than those of  $\sin^2 \theta_{23}$  and  $\sin^2 \theta_{13}$ , which is a general property of the RG evolution [29, 30], consequently the deviation from its TB value can be large. In the case of NH spectrum and large  $\tan \beta$ ,  $\sin^2 \theta_{12}$  is within the  $3\sigma$  limit only for smaller values of neutrino mass. Taking into account the lower bound on the lightest neutrino mass,  $m_{\nu 1}$  is constrained to lie in certain region, which decreases with  $\tan \beta$ . This point can be clearly seen from Fig.1. For IH spectrum, the RG effect of  $\theta_{12}$  is even larger due to the nearly degeneracy of  $m_{\nu 1}$  and  $m_{\nu 2}$ . For example, for  $\tan \beta = 10$ ,  $\sin^2 \theta_{12}$  is very close or above the  $3\sigma$  upper bound in the allowed region of  $m_{\nu 3}$ , and the values of  $\sin^2 \theta_{12}$  goes completely beyond the  $3\sigma$  limit for larger  $\tan \beta$ . As a result, the IH spectrum is strongly disfavored for  $\tan \beta > 10$  in the BMM model. We note that possible large deviation of solar neutrino mixing angle from the TB value, and small change of atmospheric and reactor angles under RG running are predicted as well in the Altarelli-Feruglio  $A_4$  model [38]. In Ref.[38], the authors perform a general analysis of running effects on lepton mixing parameters in flavor models with type I see-saw, they show that, for the mass-independent mixing pattern, the running contribution from the neutrino Yukawa coupling  $Y_\nu$  can be absorbed by a small shift on neutrino mass eigenvalues leaving mixing angles unchanged, consequently the RG change of mixing angle is due to the contribution coming from the charged lepton sector. This is exactly the reason why similar results to the  $A_4$  model are obtained here.

The variations of Majorana phases  $\varphi_1$  and  $\varphi_2$ , Dirac CP violating phase  $\delta$  and the Jarlskog invariant  $J_{CP}$  with respect to the lightest neutrino mass are also plotted in Fig. 2. We note that Dirac phase  $\delta$  arises from the running effect, even though it is undetermined in the beginning. The initial value of Jarlskog invariant  $J_{CP}$  is zero due to the vanishing of the  $\theta_{13}$  in TB mixing scheme, and it remains small because of the smallness of the  $\theta_{13}$ , although the value of  $\delta$  is large. It is remarkable that we can understand the dependence on the sign of  $\sin \Omega$  exactly. At initial scale, the right-handed neutrino mass matrix  $M_N$  shown in Eq.(15) is complex with each other for  $\sin \Omega > 0$  and  $\sin \Omega < 0$  apart from the irrelevant overall phase, and the neutrino Yukawa coupling matrix  $Y_\nu$  can be chosen to be real. Therefore, in the case of  $\sin \Omega < 0$ , the complex conjugates of  $Y_\nu$ ,  $Y_e$ ,  $M_N$  and  $\kappa$  run in the same way as the corresponding quantities of  $\sin \Omega > 0$  with the same initial conditions. Consequently the resulting low energy effective neutrino mass matrix for  $\sin \Omega < 0$  is the complex conjugate of the corresponding one of  $\sin \Omega > 0$ . As a result, the RG evolution of mixing angles and  $J_{CP}$  is independent of the sign of  $\sin \Omega$ , and summation of the each CP phase for  $\sin \Omega > 0$  and  $\sin \Omega < 0$  is equal to  $2\pi$ . These results have been confirmed in our numerical analysis explicitly.

Concretely the running of neutrino masses and mixing parameters with the energy scale is displayed in Fig. 3 for both NH and IH spectrum with  $\tan \beta = 10$ , where the initial conditions for the NH and IH are chosen to be  $m_1 = 0.041$  eV,  $\Delta m_{\text{sol}}^2 = 1.76 \times 10^{-4} \text{eV}^2$ ,  $\Delta m_{\text{atm}}^2 = 5.85 \times 10^{-3} \text{eV}^2$  and  $m_3 = 0.0538$  eV,  $\Delta m_{\text{sol}}^2 = 1.87 \times 10^{-4} \text{eV}^2$ ,  $\Delta m_{\text{atm}}^2 = 5.58 \times 10^{-3} \text{eV}^2$  respectively. Reasonable values for the lower energy oscillation parameters are reached. We see that the deviation of the solar neutrino mixing angle  $\theta_{12}$  from the TB value can be relative large for the IH spectrum, the mixing angles  $\theta_{23}$  and  $\theta_{13}$  and the CP phases  $\delta$ ,  $\varphi_1$  and  $\varphi_2$  are stable under the RG evolution, the corresponding RG corrections are small. Since  $Y_\nu^\dagger Y_\nu = y^2 \mathbf{1}$ , the contribution from the neutrino Yukawa coupling is universal above the see-saw threshold. Then, only the charged lepton relevant part  $Y_e^\dagger Y_e$  contributes to the change in mixing angles, and the evolution above the see-saw scales is essentially the same as below. This is in contrast with the usual situation where the neutrino Yukawa coupling plays dominant role in the running of neutrino mass matrix above the highest see-saw scale. Furthermore, we find that the running of

the neutrino mass  $m_{\nu i}$  is approximately given by a common scaling of the mass eigenvalues, this is the same as the situation below the see-saw scale [29, 39]. It is remarkable that the neutrino mass is reduced by about 2.4 times at low energy. We note that the above results about the running behavior of neutrino masses and mixing parameters are very general, they almost do not depend on the initial conditions.

## 4.2 RG effects in the $S_4$ model of Ding

It is remarkable that the heavy right-handed neutrinos are degenerate at LO, and the corrections to the degeneracy arising from RG running turn out to be so small that could be neglected, consequently the threshold effects should be very small in this case. In particular, we note that  $Y_\nu^\dagger Y_\nu$  is not proportional to the unit matrix any more, large RG effects seem possible. As has been demonstrated in Eq.(37), the right-handed neutrino mass  $M$  is estimated to be of order  $10^{12} \sim 10^{13} \text{ GeV}$ . Without loss of generality, we shall choose  $M = 10^{12} \text{ GeV}$  in the following numerical analysis, and we have checked that final results change very slowly with the parameter  $M$ . The neutrino mixing angles at electroweak scale as functions of the lightest neutrino mass are shown in Fig.4, it is obvious that the lightest neutrino mass for NH spectrum is bounded from below, and the lower bound on the lightest neutrino mass in the case of IH spectrum is still approximately zero. We see that the RG effects on both atmospheric and reactor angles are rather small, and the running of  $\theta_{12}$  can be large depending on  $\tan\beta$  and the mass degeneracy. Matching  $\theta_{12}$  with the data already puts strong constraints on the lightest neutrino mass spectrum and  $\tan\beta$  at the present stage, and a upper bound on the lightest neutrino mass is usually implied for small value of  $\tan\beta$ , which means that the neutrino mass spectrum can not be highly degenerate. In the case of  $\tan\beta = 20$ , the IH spectrum is ruled out, since the value of  $\sin^2\theta_{12}$  is much larger than its  $3\sigma$  upper bound. While the model is within the  $3\sigma$  limit only for small neutrino mass for NH spectrum, as is displayed in Fig.4. The predictions for the CP phases and the Jarlskog invariant are plotted in Fig.5. In a similar way as section 4.1, we learn that the evolutions of mixing angles and  $J_{CP}$  do not depend on the sign of  $\sin\Delta$ , the summation of each CP phase for  $\sin\Delta > 0$  and  $\sin\Delta < 0$  is equal to  $2\pi$ . These points are checked by our detailed numerical analysis.

The running of neutrino masses and mixing parameters with the energy scale are plotted in Fig.6. Being similar to the situation in the BMM model, the RG corrections to the CP phases  $\delta$ ,  $\varphi_1$  and  $\varphi_2$  are typically small, the corresponding curves are almost straight lines. We see that the neutrino mixing angles are rather stable under RG evolution except the solar angle for IH spectrum. The running of neutrino mass can be approximately described by a common scaling factor, and it reduced by about 2 times at electroweak scale. In short summary, the evolution of the neutrino parameters in Ding's  $S_4$  model is very similar to that of BMM model, although the textures of the mass matrices are totally different.

## 5 Conclusion

Flavor models based on discrete flavor symmetry are particularly interesting, they can produce the tri-bimaximal neutrino mixing (or some other mass-independent mixing patterns) at LO in an elegant way. It is a common feature that the LO predictions would be corrected by the subleading higher dimensional operators, and it have been shown that the subleading corrections are under control in some consistent flavor models. Since the tri-bimaximal mixing is predicted

at high energy scale, it is very necessary to investigate whether the RG effects would push the mixing parameters beyond the current allowed ranges by experimental data.

In this paper, we have analyzed the RG running of the neutrino mass and mixing parameters in the BMM model and the  $S_4$  model of Ding, both models predict tri-bimaximal neutrino mixing at LO, but the textures of the mass matrices are totally different. To study the running effects, we use the Mathematica package REAP. By detailed numerical analysis, we find that the evolution of neutrino mixing parameters displays approximately the same pattern in both  $S_4$  models. We see that the atmospheric and reactor neutrino mixing angles are essentially stable under RG evolution for both NH and IH spectrum. However, the running of solar neutrino mixing angle depends on the neutrino mass and the parameter  $\tan \beta$ , and the deviation from its TB value could be large. After we take into account the RG effects, the neutrino mass spectrum is strongly constrained by the current data on  $\theta_{12}$ , the lightest neutrino mass is bounded from both below and up, and the upper bound decreases with  $\tan \beta$ . For large  $\tan \beta$  ( $\tan \beta > 10$ ), the value of  $\sin^2 \theta_{12}$  could be larger than its  $3\sigma$  upper bound for the whole spectrum in the case of IH spectrum. As a result, the IH neutrino mass spectrum is disfavored in the case of large  $\tan \beta$ . Moreover, we note that the running of light-neutrino masses can be approximately described by a common scaling factor, and they reduce by about  $1.2 \sim 3$  times at low energy. This effects is neglected in Ref.[38]. We note that the evolutions of mixing angles and  $J_{CP}$  don't depend on the sign of  $\sin \Omega$  or  $\sin \Delta$ , and the sum of each CP phase for both sign is equal to  $2\pi$ . These results are confirmed both analytically and numerically.

Finally we note that running of neutrino parameters in the Altarelli-Feruglio  $A_4$  model, BMM model and Ding's  $S_4$  model is similar to each other, although they produce tri-bimaximal mixing in different ways. The reason is that the neutrino Yukawa coupling only contributes to the running of neutrino mass, it doesn't affect the lepton mixing angles, and the change in mixing angles is due to the contribution from the charged lepton sector. We conclude that the running of mixing parameters is also severely constrained by the flavor symmetry in discrete flavor symmetry models.

## Acknowledgements

We are grateful to Prof. Zhi-Zhong Xing for stimulating discussions on RGE running. The author Gui-Jun Ding gratefully acknowledge the pleasant hospitality of the theory group at the University of Wisconsin. This work is supported by the National Natural Science Foundation of China under Grant No.10905053, Chinese Academy KJCX2-YW-N29 and the 973 project with Grant No. 2009CB825200. Dong-Mei Pan is supported in part by the National Natural Science Foundation of China under Grant No.10775124.

## References

- [1] A. Strumia and F. Vissani, arXiv:hep-ph/0606054; M. C. Gonzalez-Garcia and M. Maltoni, Phys. Rept. **460**, 1 (2008) [arXiv:0704.1800 [hep-ph]].
- [2] T. Schwetz, M. Tortola and J. W. F. Valle, arXiv:1103.0734 [hep-ph]; T. Schwetz, M. A. Tortola and J. W. F. Valle, New J. Phys. **10**, 113011 (2008) [arXiv:0808.2016 [hep-ph]]; M. Maltoni and T. Schwetz, arXiv:0812.3161 [hep-ph].

- [3] G. L. Fogli, E. Lisi, A. Marrone, A. Palazzo and A. M. Rotunno, arXiv:0809.2936 [hep-ph]; G. L. Fogli, E. Lisi, A. Marrone, A. Palazzo and A. M. Rotunno, Phys. Rev. Lett. **101** (2008) 141801 [arXiv:0806.2649 [hep-ph]].
- [4] P. F. Harrison, D. H. Perkins and W. G. Scott, Phys. Lett. B **530**, 167 (2002), hep-ph/0202074; P. F. Harrison and W. G. Scott, Phys. Lett. B **535**, 163 (2002), hep-ph/0203209; Z. Z. Xing, Phys. Lett. B **533**, 85 (2002), hep-ph/0204049; X. G. He and A. Zee, Phys. Lett. B **560**, 87 (2003), hep-ph/0301092.
- [5] G. Altarelli and F. Feruglio, Rev. Mod. Phys. **82**, 2701 (2010) [arXiv:1002.0211 [hep-ph]].
- [6] H. Ishimori, T. Kobayashi, H. Ohki, H. Okada, Y. Shimizu and M. Tanimoto, Prog. Theor. Phys. Suppl. **183**, 1 (2010) [arXiv:1003.3552 [hep-th]].
- [7] K. R. S. Balaji, A. S. Dighe, R. N. Mohapatra and M. K. Parida, Phys. Lett. B **481**, 33 (2000) [arXiv:hep-ph/0002177]; S. Antusch and M. Ratz, JHEP **0211**, 010 (2002) [arXiv:hep-ph/0208136]; R. N. Mohapatra, M. K. Parida and G. Rajasekaran, Phys. Rev. D **69**, 053007 (2004) [arXiv:hep-ph/0301234].
- [8] S. Antusch, J. Kersten, M. Lindner and M. Ratz, Phys. Lett. B **544**, 1 (2002) [arXiv:hep-ph/0206078]; T. Miura, T. Shindou and E. Takasugi, Phys. Rev. D **68**, 093009 (2003) [arXiv:hep-ph/0308109].
- [9] F. Bazzocchi, L. Merlo and S. Morisi, Nucl. Phys. B **816**, 204 (2009) [arXiv:0901.2086 [hep-ph]]; F. Bazzocchi, L. Merlo and S. Morisi, Phys. Rev. D **80**, 053003 (2009) [arXiv:0902.2849 [hep-ph]].
- [10] G. J. Ding, Nucl. Phys. B **827**, 82 (2010) [arXiv:0909.2210 [hep-ph]].
- [11] C. S. Lam, Phys. Rev. Lett. **101**, 121602 (2008) [arXiv:0804.2622 [hep-ph]]; C. S. Lam, Phys. Rev. D **78**, 073015 (2008) [arXiv:0809.1185 [hep-ph]]; C. S. Lam, arXiv:0907.2206 [hep-ph].
- [12] E. Ma, Phys. Lett. B **632**, 352 (2006) [arXiv:hep-ph/0508231].
- [13] D. Meloni, J. Phys. G **37**, 055201 (2010) [arXiv:0911.3591 [hep-ph]].
- [14] G. Altarelli, F. Feruglio and L. Merlo, JHEP **0905**, 020 (2009) [arXiv:0903.1940 [hep-ph]].
- [15] W. Grimus, L. Lavoura and P. O. Ludl, J. Phys. G **36**, 115007 (2009) [arXiv:0906.2689 [hep-ph]].
- [16] B. Dutta, Y. Mimura and R. N. Mohapatra, JHEP **1005**, 034 (2010) [arXiv:0911.2242 [hep-ph]].
- [17] C. Hagedorn, S. F. King and C. Luhn, JHEP **1006**, 048 (2010) [arXiv:1003.4249 [hep-ph]].
- [18] H. Ishimori, Y. Shimizu and M. Tanimoto, Prog. Theor. Phys. **121**, 769 (2009) [arXiv:0812.5031 [hep-ph]]; H. Ishimori, K. Saga, Y. Shimizu and M. Tanimoto, arXiv:1004.5004 [hep-ph].

- [19] R. de Adelhart Toorop, F. Bazzocchi and L. Merlo, JHEP **1008**, 001 (2010) [arXiv:1003.4502 [hep-ph]].
- [20] G. J. Ding, Nucl. Phys. B **846**, 394 (2011) [arXiv:1006.4800 [hep-ph]].
- [21] S. Pakvasa and H. Sugawara, Phys. Lett. B **82**, 105 (1979); T. Brown, N. Deshpande, S. Pakvasa and H. Sugawara, Phys. Lett. B **141**, 95 (1984); Y. Yamanaka, H. Sugawara and S. Pakvasa, Phys. Rev. D **25**, 1895 (1982) [Erratum-ibid. D **29**, 2135 (1984)]; T. Brown, S. Pakvasa, H. Sugawara and Y. Yamanaka, Phys. Rev. D **30**, 255 (1984).
- [22] D. G. Lee and R. N. Mohapatra, Phys. Lett. B **329**, 463 (1994) [arXiv:hep-ph/9403201]; C. Hagedorn, M. Lindner and R. N. Mohapatra, JHEP **0606**, 042 (2006) [arXiv:hep-ph/0602244]; Y. Cai and H. B. Yu, Phys. Rev. D **74**, 115005 (2006) [arXiv:hep-ph/0608022]; H. Zhang, Phys. Lett. B **655**, 132 (2007) [arXiv:hep-ph/0612214]; Y. Koide, JHEP **0708**, 086 (2007) [arXiv:0705.2275 [hep-ph]]; M. K. Parida, Phys. Rev. D **78**, 053004 (2008) [arXiv:0804.4571 [hep-ph]].
- [23] P. H. Chankowski and Z. Pluciennik, Phys. Lett. B **316**, 312 (1993) [arXiv:hep-ph/9306333]; K. S. Babu, C. N. Leung and J. T. Pantaleone, Phys. Lett. B **319**, 191 (1993) [arXiv:hep-ph/9309223].
- [24] J. A. Casas, J. R. Espinosa, A. Ibarra and I. Navarro, Nucl. Phys. B **569**, 82 (2000) [arXiv:hep-ph/9905381]; J. A. Casas, J. R. Espinosa, A. Ibarra and I. Navarro, Nucl. Phys. B **573**, 652 (2000) [arXiv:hep-ph/9910420].
- [25] S. Antusch, M. Drees, J. Kersten, M. Lindner and M. Ratz, Phys. Lett. B **519**, 238 (2001) [arXiv:hep-ph/0108005]; S. Antusch, J. Kersten, M. Lindner and M. Ratz, Phys. Lett. B **538**, 87 (2002) [arXiv:hep-ph/0203233]; M. Lindner, M. A. Schmidt and A. Y. Smirnov, JHEP **0507**, 048 (2005) [arXiv:hep-ph/0505067].
- [26] S. F. King and N. N. Singh, Nucl. Phys. B **591**, 3 (2000) [arXiv:hep-ph/0006229]; J. w. Mei, Phys. Rev. D **71**, 073012 (2005) [arXiv:hep-ph/0502015]; J. R. Ellis, A. Hektor, M. Kadastik, K. Kannike and M. Raidal, Phys. Lett. B **631**, 32 (2005) [arXiv:hep-ph/0506122].
- [27] W. Chao and H. Zhang, Phys. Rev. D **75**, 033003 (2007) [arXiv:hep-ph/0611323]; M. A. Schmidt, Phys. Rev. D **76**, 073010 (2007) [arXiv:0705.3841 [hep-ph]].
- [28] J. Chakraborty, A. Dighe, S. Goswami and S. Ray, Nucl. Phys. B **820**, 116 (2009) [arXiv:0812.2776 [hep-ph]].
- [29] S. Antusch, J. Kersten, M. Lindner and M. Ratz, Nucl. Phys. B **674**, 401 (2003) [arXiv:hep-ph/0305273].
- [30] S. Antusch, J. Kersten, M. Lindner, M. Ratz and M. A. Schmidt, JHEP **0503**, 024 (2005) [arXiv:hep-ph/0501272].
- [31] Z. z. Xing, H. Zhang and S. Zhou, Phys. Rev. D **77**, 113016 (2008) [arXiv:0712.1419 [hep-ph]].



- [32] J. Bergstrom, M. Malinsky, T. Ohlsson and H. Zhang, Phys. Rev. D **81**, 116006 (2010) [arXiv:1004.4628 [hep-ph]].
- [33] M. Blennow, H. Melbeus, T. Ohlsson and H. Zhang, arXiv:1101.2585 [hep-ph].
- [34] J. Barry and W. Rodejohann, Nucl. Phys. B **842**, 33 (2011) [arXiv:1007.5217 [hep-ph]].
- [35] K. Nakamura *et al.* [Particle Data Group], J. Phys. G **37**, 075021 (2010).
- [36] S. Antusch and M. Spinrath, Phys. Rev. D **78**, 075020 (2008) [arXiv:0804.0717 [hep-ph]];  
S. Boudjemaa and S. F. King, Phys. Rev. D **79**, 033001 (2009) [arXiv:0808.2782 [hep-ph]];  
M. Bustamante, A. M. Gago and J. Jones-Perez, arXiv:1012.2728 [hep-ph].
- [37] A. Osipowicz *et al.* [KATRIN Collaboration], arXiv:hep-ex/0109033; see also:  
<http://www-ik.fzk.de/~katrin/index.html>.
- [38] Y. Lin, L. Merlo and A. Paris, Nucl. Phys. B **835**, 238 (2010) [arXiv:0911.3037 [hep-ph]].
- [39] P. H. Chankowski and S. Pokorski, Int. J. Mod. Phys. A **17**, 575 (2002)[arXiv:hep-ph/0110249].

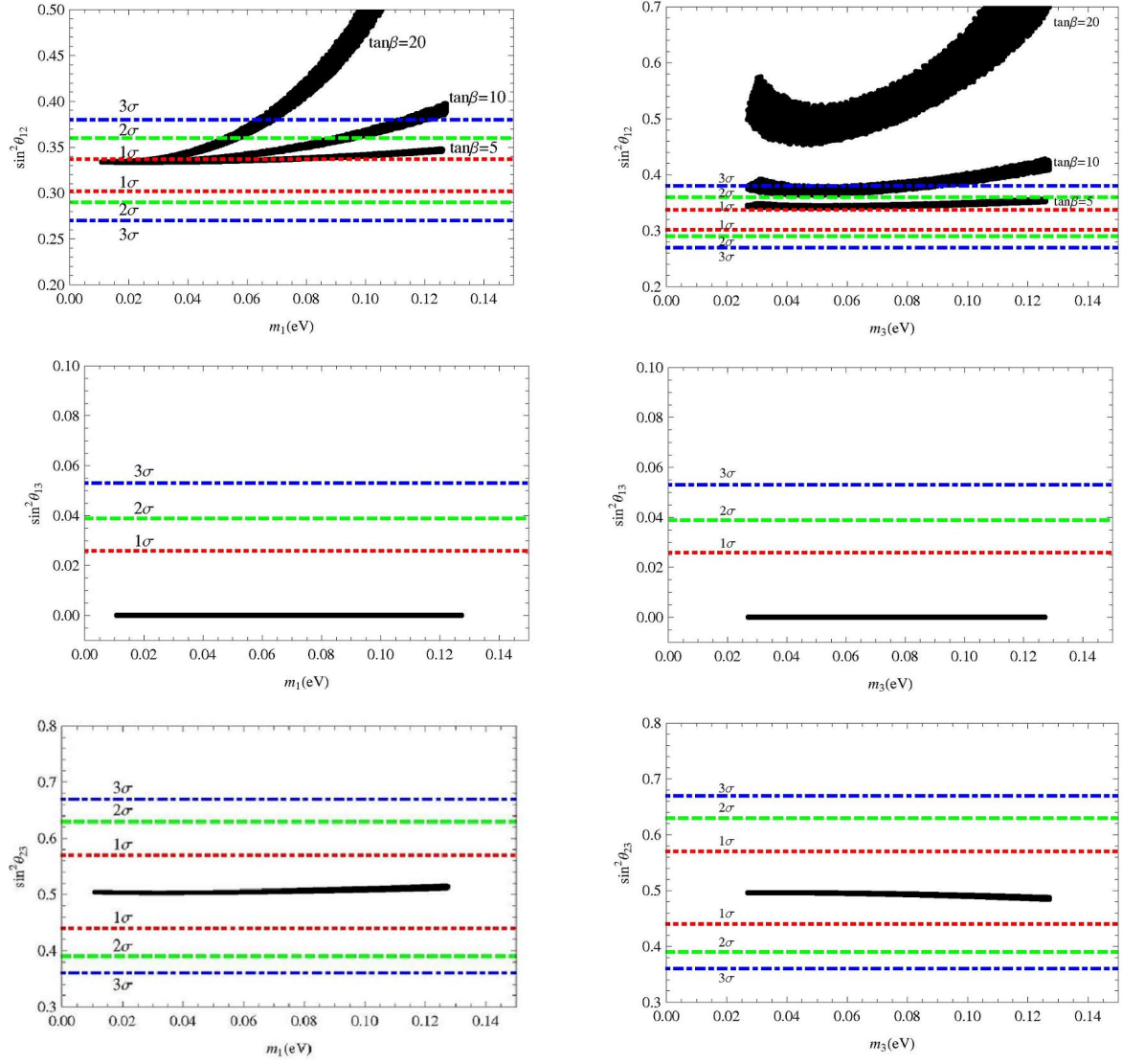


Figure 1: RGE corrections to the neutrino mixing angles in the BMM  $S_4$  model with  $\tan \beta = 10$ . The left column of the plots are the results for NH spectrum, and the right column for the IH case. In the case of  $\sin^2 \theta_{12}$ ,  $\tan \beta = 5$  and  $\tan \beta = 20$  are considered.

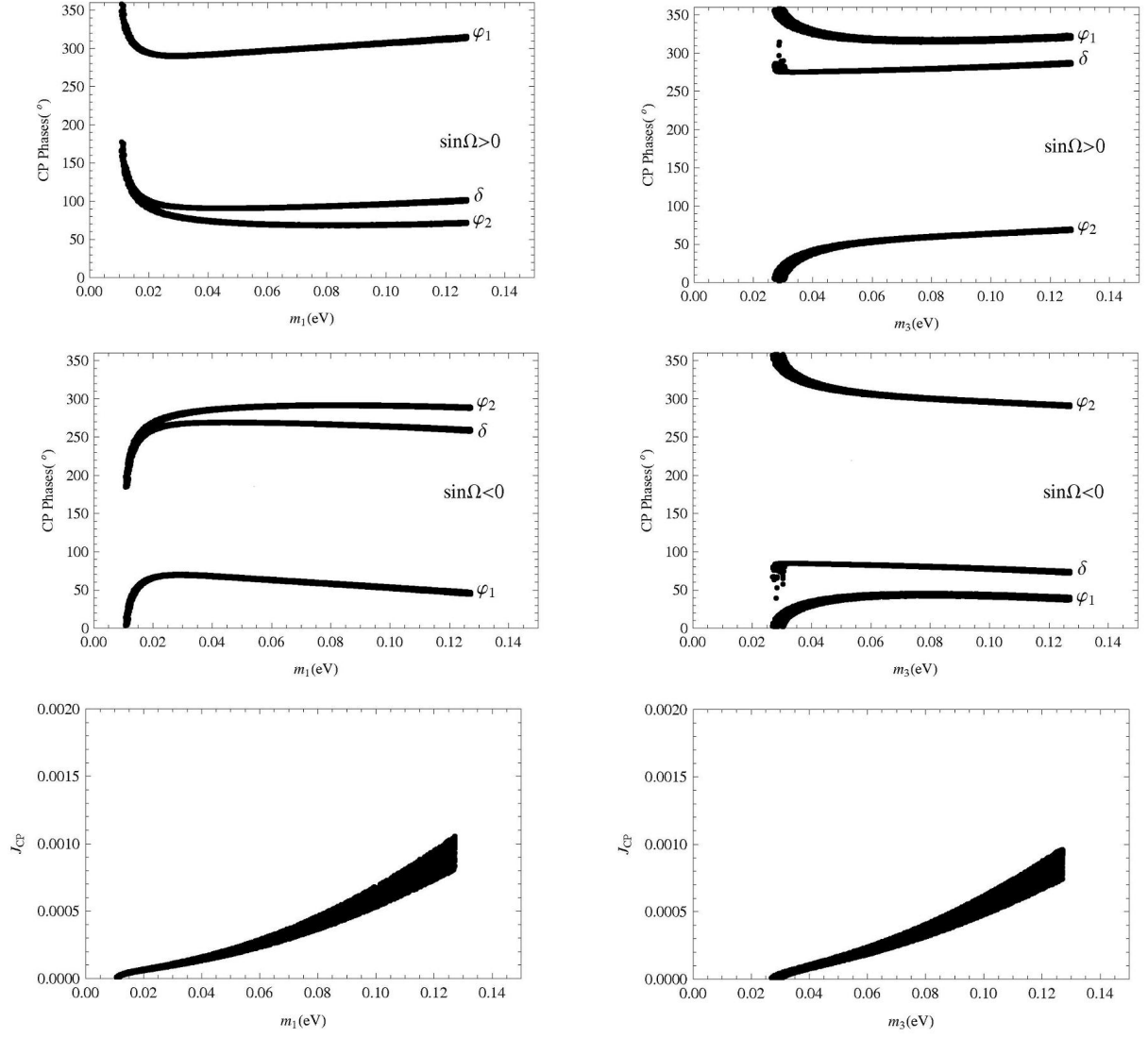


Figure 2: RGE corrections to the CP phases and the Jarlskog invariant in the BMM  $S_4$  model with  $\tan \beta = 10$ . The left column of the plots are the results for NH spectrum, and the right column for the IH case.

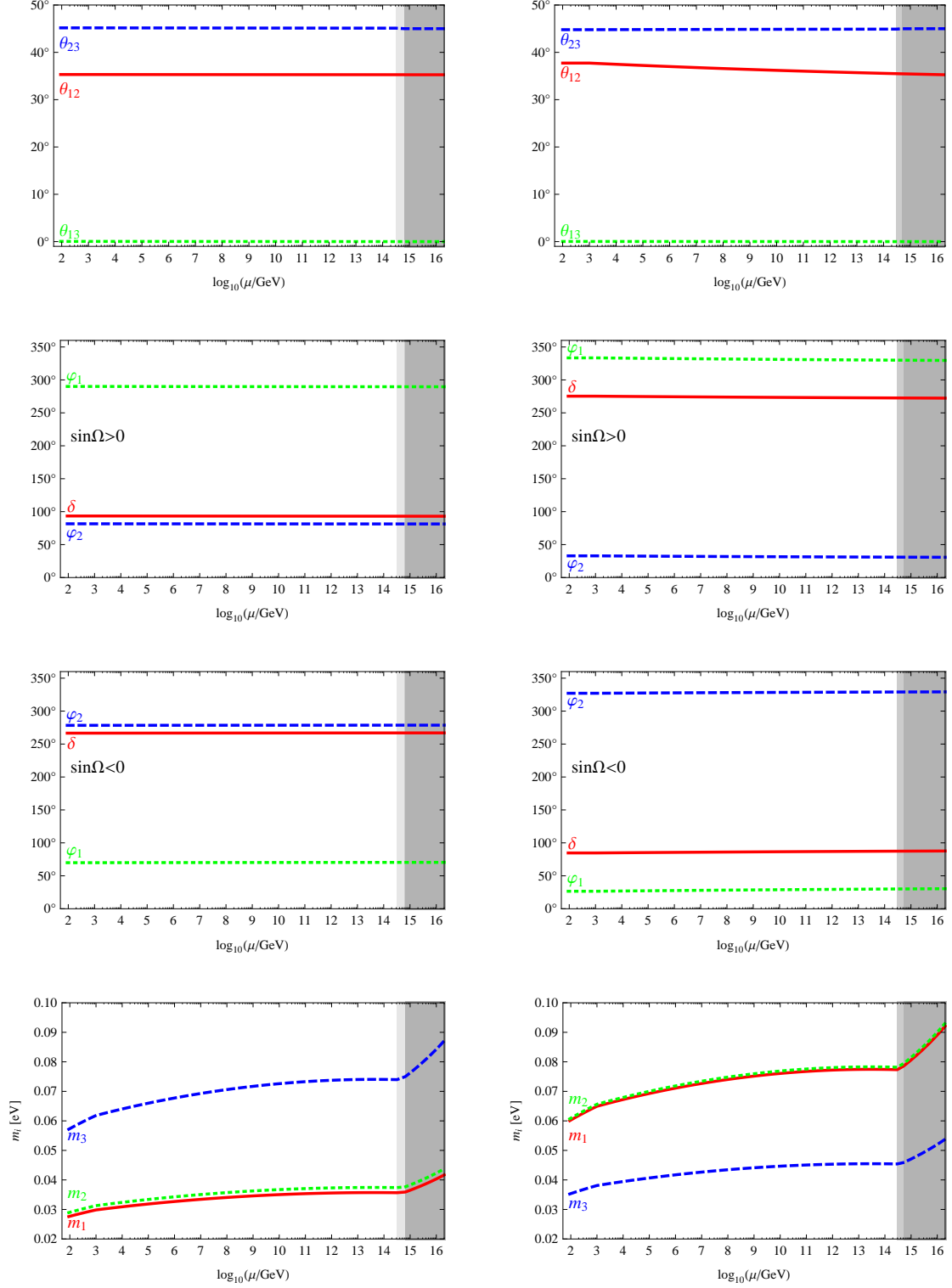


Figure 3: The running of the neutrino masses and mixing parameters with the energy scale in the BMM  $S_4$  model with  $\tan\beta = 10$  and  $M_{SUSY} = 1$  TeV. The left column is the predictions for NH spectrum with  $m_1 = 0.041$  eV,  $\Delta m_{\text{sol}}^2 = 1.76 \times 10^{-4} \text{eV}^2$  and  $\Delta m_{\text{atm}}^2 = 5.85 \times 10^{-3} \text{eV}^2$ . The right column is for the IH case with  $m_3 = 0.0538$  eV,  $\Delta m_{\text{sol}}^2 = 1.87 \times 10^{-4} \text{eV}^2$  and  $\Delta m_{\text{atm}}^2 = 5.58 \times 10^{-3} \text{eV}^2$ .

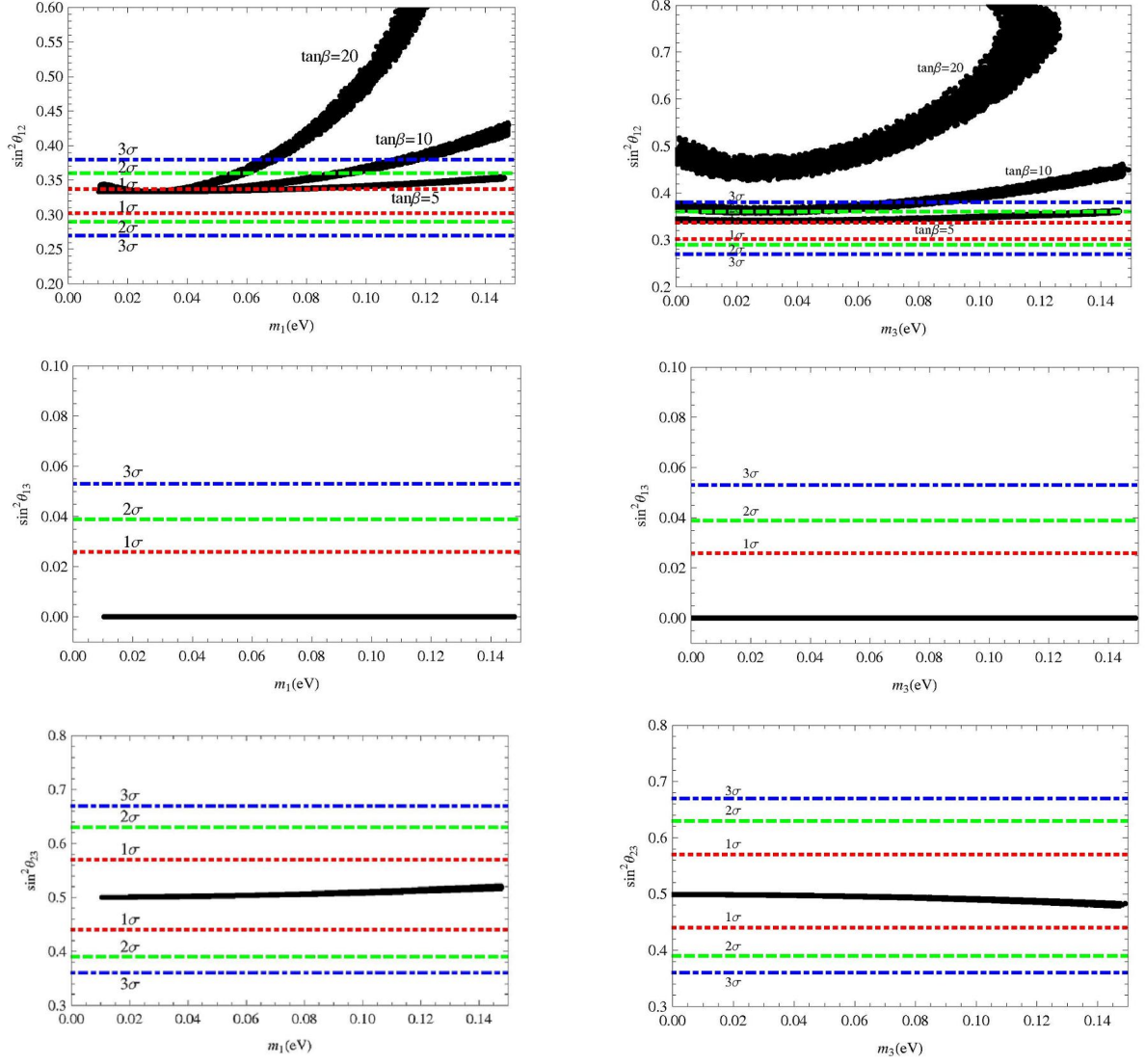


Figure 4: RGE corrections to the neutrino mixing angles in the  $S_4$  model of Ding with  $\tan \beta = 10$ . The left column of the plots are the results for NH spectrum, and the right column for the IH case. In the case of  $\sin^2 \theta_{12}$ ,  $\tan \beta = 5$  and  $\tan \beta = 20$  are considered.

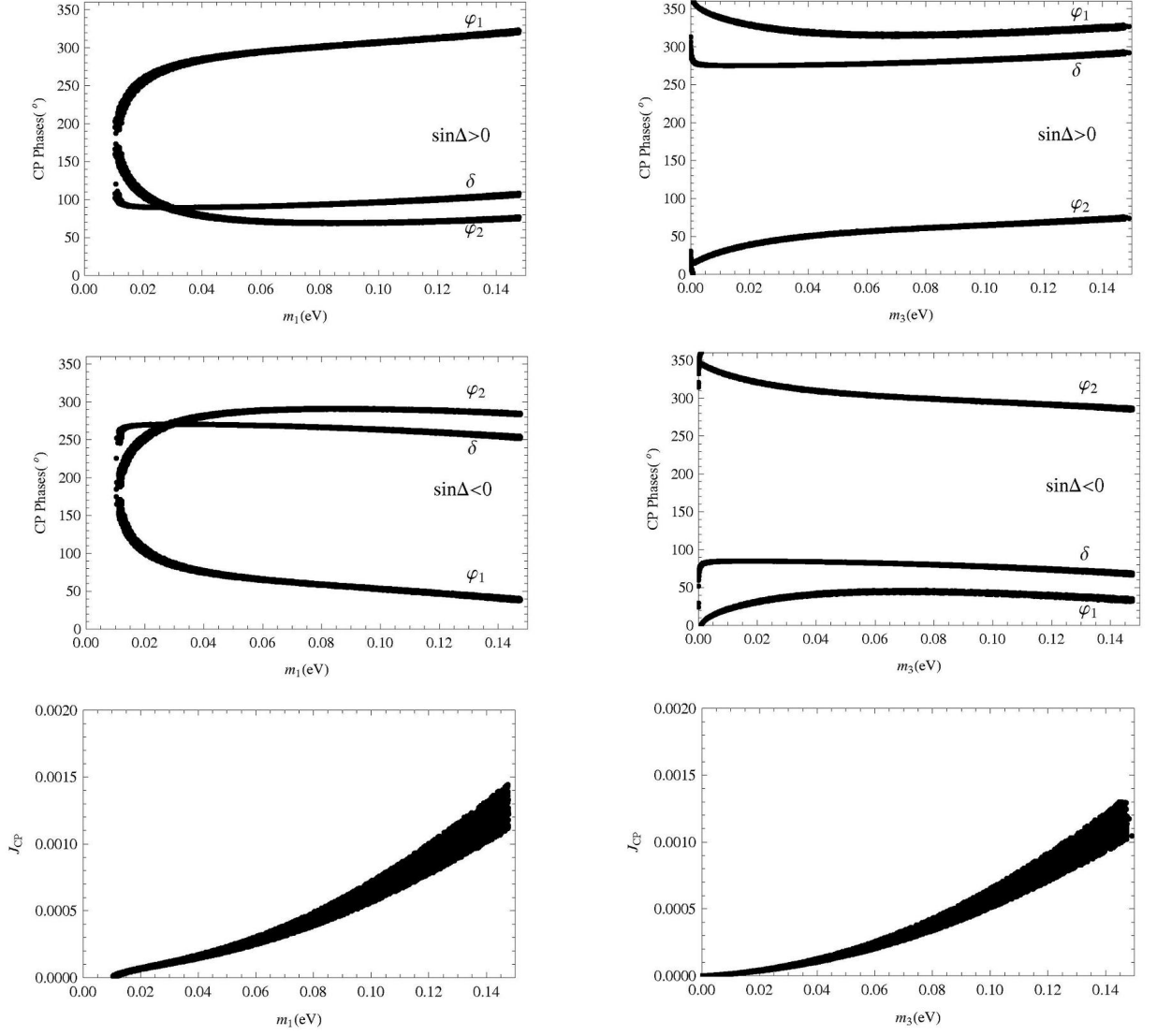


Figure 5: RGE corrections to the CP phases and the Jarlskog invariant in the  $S_4$  model of Ding with  $\tan \beta = 10$ . The left column of the plots are the results for NH spectrum, and the right column for the IH case.

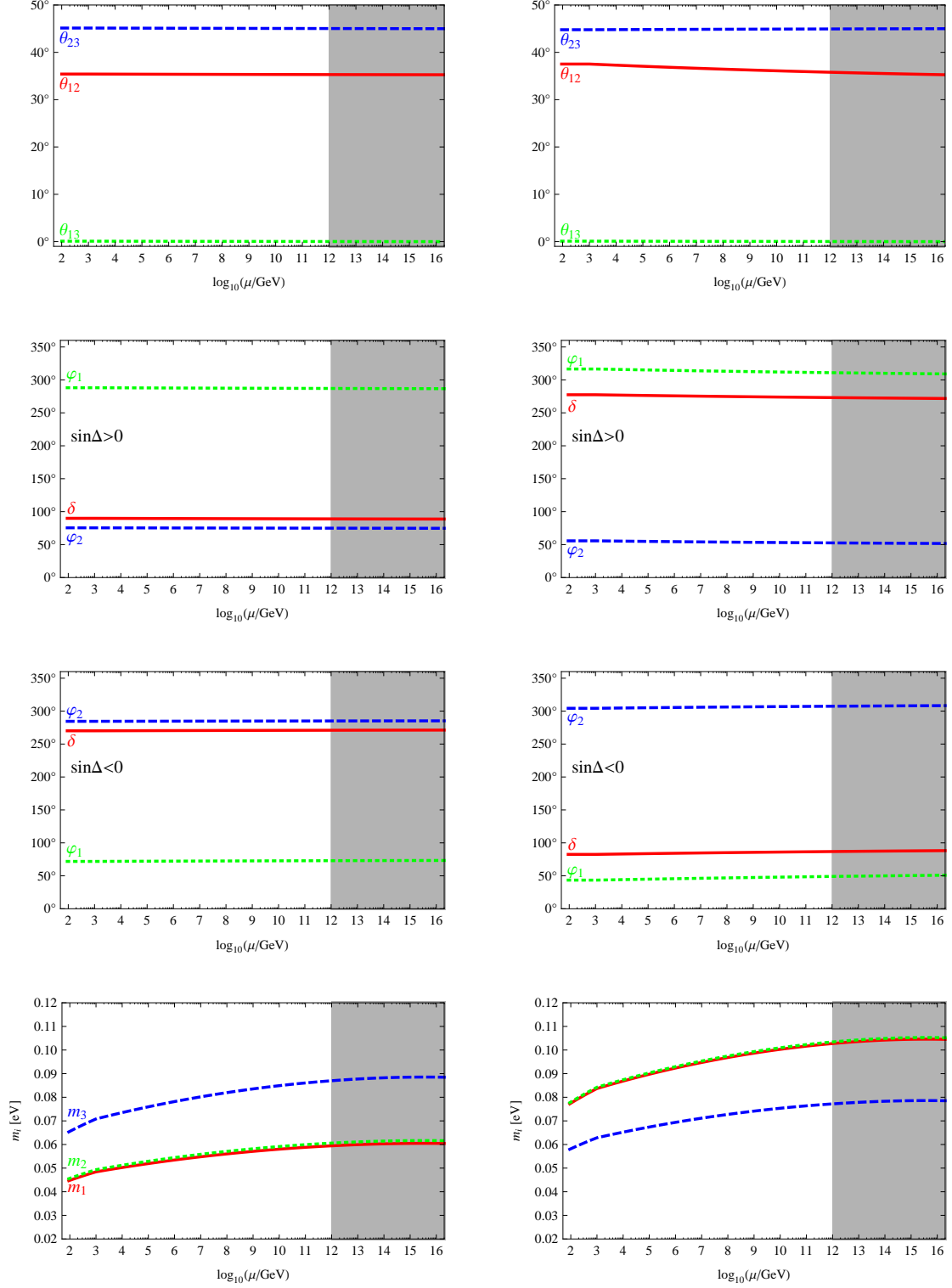


Figure 6: The running of the neutrino masses and mixing parameters with the energy scale in the  $S_4$  model of Ding with  $\tan\beta = 10$  and  $M_{SUSY} = 1$  TeV. The left column is the predictions for NH spectrum with  $m_1 = 0.0604$  eV,  $\Delta m_{\text{sol}}^2 = 1.43 \times 10^{-4} \text{eV}^2$  and  $\Delta m_{\text{atm}}^2 = 4.18 \times 10^{-3} \text{eV}^2$ . The right column is for the IH case with  $m_3 = 0.0785$  eV,  $\Delta m_{\text{sol}}^2 = 1.48 \times 10^{-4} \text{eV}^2$  and  $\Delta m_{\text{atm}}^2 = 4.75 \times 10^{-3} \text{eV}^2$ .